Prediction of Interfacial Filler Thickness for Minimum Thermal Contact Resistance

P. W. O'Callaghan,* B. Snaith,† and S. D. Probert‡
Cranfield Institute of Technology, Cranfield, England
and
F. R. Al-Astrabadi§
Servizio Studi Speciali, Aeritalia Divisione Aviazone, Torino, Italy

A theoretical optimization procedure to establish the appropriate filler thickness for minimizing thermal contact resistance between flat non-wavy surfaces is developed and demonstrated. The analysis is founded upon the assumption of ideal plastic asperity deformation at the interface formed between randomly rough surfaces separated by the softer filler material. Experimental measurements of the thermal contact resistance for various contacting assemblies are presented to verify the prediction.

Nomenclature

$\tilde{a}$ = mean radius of microcontact spot, m
A = contact area, m^2
b = radius of a heat flow channel, m
$g(Z)$ = constriction alleviation function described by Eq. (34)
k = thermal conductivity, $Wm^{-1}K^{-1}$
M = micro-indentation hardness, Nm^{-2}
$\tilde{N}$ = mean number of microcontact spots per unit area, m^{-2}
P = contact pressure, MNm^{-2}
$\dot{Q}$ = rate of heat flux crossing the interface, W
R = thermal contact resistance of unit area, KW^{-1}
t = normalized mean plane separation, $=u/\sigma$
u = mean plane separation, m
x = lateral spread of filler surrounding each metal-to-metal contact spot, Eq. (15)
y = normalized filler thickness, i.e., δ/σ
δ = thickness of filler, m
ΔT = apparent temperature discontinuity across the interface, K
$\phi(t)$ = Gaussian or normal probability function, Eq. (10)
$\Phi(t)$ = $\int_0^t \phi(t)\,dt$
ψ = asperity slope, rad or deg as specified
Ψ = $|\tilde{\psi}|/\sigma$, rad·m^{-1}
σ = surface rms roughness, m

Subscripts

* = optimal condition
an = annular-type microcontacts
av = average
f = filler
M = metal
MM = metal-to-metal
Mf,fM = metal-to-filler
o = overall
s = effective for a contact between dissimilar surfaces
tot = total
1,2 = surfaces 1 and 2, respectively

Received March 31, 1982; revision submitted Nov. 22, 1982.
Copyright © American Institute of Aeronautics and Astronautics, Inc., 1983. All rights reserved.

*Reader in Energy Management. Member AIAA.
†Research Officer. Member AIAA.
‡Professor of Applied Energy.
§Thermal Design Engineer.

Introduction

THE correct prediction of thermal contact resistance (TCR) is vital for designs involving thermal flows through spacecraft systems. In addition, it is often desirable that this resistance to heat flow be minimized in order to dissipate heat rapidly from limited area high-heat-flux components. The thermal resistances of unfilled dry, pressed contacts are notoriously unreproducible and difficult to predict. The insertion of a *soft,* high-conductivity foil or coating at the interface results in a more consistent thermal performance.[1-3] The selection of the optimal filler thickness can, in addition, minimize the TCR for a given interfacial applied loading pressure. This paper develops an analytical technique[4,5] to predict this optimal thickness. The theory is founded upon the assumption that the ideal plastic deformation behavior occurs at the interface between randomly rough surfaces and requires as input the thermophysical and topographical characteristics of the contacting surfaces. Experimental measurements of the TCR for various assemblies are presented to verify the predictions.

The existence of an optimal filler thickness for minimum thermal contact resistance is expected to occur when the filler thickness δ is of the order of the surface roughness σ. When $\delta \ll \sigma$, the constriction resistance experienced at contacting base material-to-base material asperities is alleviated by the additional thermal bridges made across the filler material. For filler thicknesses much greater than δ, the additional bulk resistance of the filler discounts the reduction in constriction resistance produced by the filler.

It must be stressed that the insertion of a filler which is harder than the base material will result in increased overall contact resistance, regardless of the thickness or thermal conductivity of the insert material.

The Prediction

The theoretical analysis developed here applies for the initial loading sequence of a virgin contact, for which it is assumed that the contacting surface microasperities deform in an ideal plastic manner. The theory also assumes that all material within the intersections of the surfaces plays no further part in influencing the behavior as normal loading proceeds. It is further assumed that the filler material also deforms in an ideal plastic manner. If the filler were fully ductile, it would extrude from the asperity intersections into noncontact regions and, under conditions of ideal plastic deformation, would result in lower values of thermal contact resistance than the prediction suggests. This effect would be particularly enhanced in the region of the optimum.

The following approximations are also introduced:

1) Surface asperities may be represented as right circular cones.

2) All microcontact regions are annular.

3) The filler is of uniform thickness and so its presence does not alter the surface topographies.

4) As a result of assumptions 2 and 3 the contact configuration found at contacting surfaces separated by a filler is comprised of base-material to base-material annular microcontacts surrounded by concentric circular annuli of the filler material, with additional circular microcontacts of the filler material alone.

5) The height distributions of the contact surfaces may be described by Gaussian probability functions.

6) The effective thermal conductivity of a filler-to-filler microcontact is given by the harmonic mean of the conductivities of the filler and base material, respectively.

7) The effective thermal conductivity of an "annular type" contact, described in assumption 4, is given by the arithmetic mean of the conductivities of the base material and filler.

Analysis

When surfaces are pressed together, sandwiching a secondary material at the interface, the demographic characteristics of the resulting microcontact spots differ from those that occur in the absence of the filler.

A previous analysis,[6,7] which led to a prediction of the thermal behavior of oxidized contacts, presented the following classifications for filled contacts.

If the filler is softer than the base contact material, a greater real area of contact will be produced under a specified interfacial loading pressure. Then the degree of improvement in the thermal conductance also depends upon the ratio of the thermal conductivities of the filler and base materials. The thickness of the insert material δ relative to the rms roughness σ of the primary contacting surfaces is the most influential parameter.

1) When $\delta \gg \sigma$, assuming that the filler material is incompressible, then the TCR always increases with increasing δ according to the linear one-dimensional definition

$$\Delta R = \Delta\delta / k_f \tag{1}$$

where k_f is the effective conductivity of the insert material.

2) When δ is of the order of, or less than, σ and the filler is softer than the primary contact material, a decreased TCR will occur for all loads such that the mean plane separation of the base material surfaces u_M is greater than δ, regardless of the ratio of thermal conductivities. The conductance of each primary microcontact is enhanced by additional annular bridges of filler material surrounding each primary microcontact, as well as independent microcontacts that occur through the filler alone.

3) Because, under constant load, the TCR reduces with increasing δ for $\delta < \sigma$ and increases with increasing δ for $\delta \gg \sigma$ a minimum value of TCR will be encountered when δ is of the order of σ. This minimum value corresponds to the situation resulting when the filler is sufficiently thick so that no base material-to-base material microcontacts form, the applied loading pressure being accommodated by flow stresses in the filler material alone. The exact filler thickness to produce this optimal resistance is difficult to predict mathematically because of the uncertainties regarding the degrees of plasticity and ductility and because it involves the simultaneous solution of two complex mechanisms of heat conductance. Three additional indices affect the thermal behavior of filled contacts:

$$\frac{\text{Filler hardness}}{\text{Primary material hardness}} = \frac{M_f}{M_M} \tag{2}$$

$$\frac{\text{Filler thermal conductivity}}{\text{Primary material thermal conductivity}} = \frac{k_f}{k_M} \tag{3}$$

and

$$\frac{\text{Filler thickness}}{\text{Effective rms roughness of unfilled joint}} = \frac{\delta}{\sigma} \tag{4}$$

For a randomly rough surface in contact with a flat surface of the same material, assuming ideal plastic deformation,[2,4-7] the following analysis applies.

1) When no filler is present (Fig. 1a), the TCR can be estimated from

$$R_o' = (2\overline{a_M} \bar{N}_M k_M)^{-1} \tag{5}$$

where

$$\overline{a_M} = 2/\pi \Psi t_M \tag{6}$$

$$\bar{N}_M = \Psi^2 \pi t_M \phi(t_M)/8 \tag{7}$$

$$\Psi = |\bar{\psi}|/\sigma \tag{8}$$

$$t_M = u_M/\sigma \tag{9}$$

$$\phi(t_M) = (1/\sqrt{2\pi}) e^{-t_M^2/2} \tag{10}$$

where u_M is the mean surface separation, $|\bar{\psi}|$ the mean absolute surface slope, and k_M the thermal conductivity of the base material.

The normalized mean plane separation t_M is related to the normal applied loading pressure P by

$$\Phi(t_M) = \frac{1}{2} - \frac{P}{M_M} = \frac{1}{\sqrt{2\pi}} \int_0^{t_M} e^{-t_M^2/2} dt_M \tag{11}$$

2) When a filler of thickness δ, less than the order of magnitude of the roughness σ, is present at the interface, the

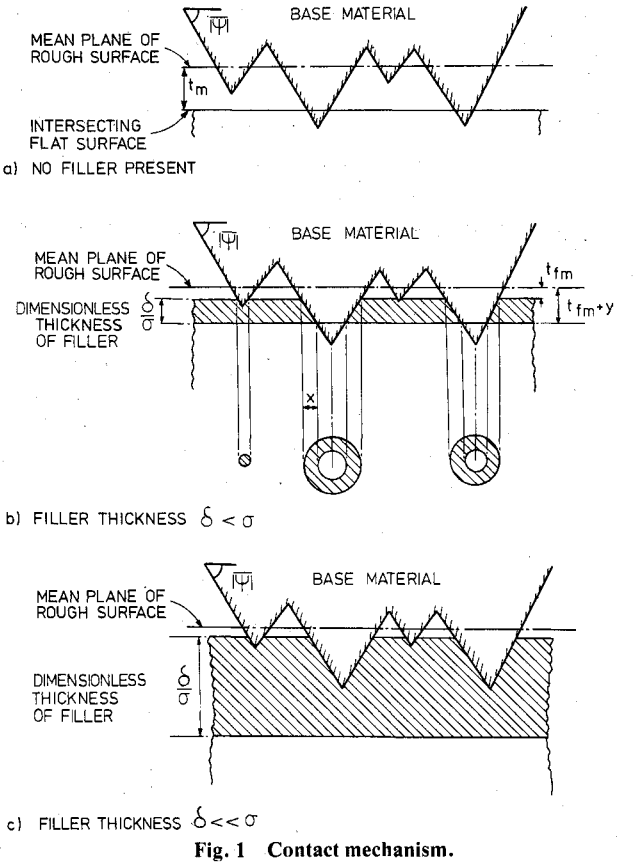

Fig. 1 Contact mechanism.

prediction of the TCR is similar to that outlined previously[6] for oxidized contacts. The applied load is supported by the base material-to-base material as well as the base material-to-filler microcontacting areas. If u_{fM} is the mean plane separation between the rough base material surface and the filler surface nearer this rough surface (Fig. 1b), then

$$t_{fM} = u_{fM}/\sigma \tag{12}$$

and can be estimated from

$$\left[\frac{1}{2} - \Phi(t_{fM}+y)\right] + [\Phi(t_{fM}+y) - \Phi(t_{fM})]\,\frac{M_f}{M_M} = \frac{P}{M_M} \tag{13}$$

where

$$y = \delta/\sigma \tag{14}$$

Two types of thermally constricting microcontact area occur:

a) $\bar{N}_{MM}$ base material-to-base material microcontacts of mean radius $\bar{a}_{MM}$ surrounded by annuli of the filler of lateral extent

$$x = \delta/\sigma \tan|\bar{\psi}| \tag{15}$$

each having a mean effective thermal conductivity given by

$$k_{av} = (k_M + k_f)/2 \tag{16}$$

b) $\bar{N}_{Mf}$ microcontacts of mean radius $\bar{a}_{Mf}$ formed between the base material and filler, each having a mean effective thermal conductivity given by

$$2/k_{Mf} = (1/k_M) + (1/k_f) \tag{17}$$

Now

$$\bar{N}_{tot} = \Psi^2 \pi t_{fM} \phi(t_{fM})/8 \tag{18}$$

$$\bar{a}_{tot} = 2/\pi\Psi t_{fM} \tag{19}$$

$$\bar{a}_{MM} = 2/\pi\Psi(t_{fM}+y) \tag{20}$$

$$\bar{N}_{MM} = \Psi^2 \pi (t_{fM}+y)\phi(t_{fM}+y)/8 = \bar{N}_{an} \tag{21}$$

$$\bar{N}_{Mf} = \bar{N}_{tot} - \bar{N}_{MM} \tag{22}$$

and

$$\bar{a}_{an} = \bar{a}_{MM} + x\sigma \tag{23}$$

For a linear intersection of the contact plane,

$$\bar{a}_{Mf} = \frac{\bar{N}_{tot}\bar{a}_{tot} - \bar{N}_{MM}\bar{a}_{an}}{\bar{N}_{Mf}} \tag{24}$$

Then, the constriction resistance of the microcontacts, comprising the base material surrounded by annuli of the filler, is given by

$$R'_{an} = (2\bar{a}_{an}\bar{N}_{MM}k_{av})^{-1} \tag{25}$$

and the resistance of the base material-to-filler by

$$R'_{Mf} = (2\bar{a}_{Mf}\bar{N}_{Mf}k_{Mf})^{-1} \tag{26}$$

Then the total contact resistance of unit nominal contact area is calculated from

$$1/R'_{\delta<\sigma} = (1/R'_{an}) + (1/R'_{Mf}) \tag{27}$$

At the optimal thickness δ^*, the TCR of the unit area is calculated from

$$R'^* = (2\bar{a}^*_{Mf}\bar{N}^*_{Mf}k_{Mf})^{-1} \tag{28}$$

i.e., as for the contact in the absence of the filler, but the mean plane separation now depends upon the hardness of the filler, viz,

$$\Phi(t^*_{Mf}) = \tfrac{1}{2} - P/M_f \tag{29}$$

3) For $\delta \gg \sigma$ (Fig. 1c), the TCR increases according to

$$\Delta TCR = \Delta\delta/k_f \tag{30}$$

In order to predict the behavior of the filled contact formed between two surfaces 1 and 2 of the same material, but having different surface topographies, certain compound parameters (σ_s, t_s, and y_s) are used. This permits the actual contact configuration to be represented as a statistically equivalent assembly between a perfectly flat smooth surface and a rough surface, i.e.,

$$\sigma_s = (\sigma_1^2 + \sigma_2^2)^{0.5} \tag{31}$$

Then

$$t_s = u/\sigma_s \tag{32}$$

$$y_s = \delta/\sigma_s \tag{33}$$

The constriction alleviation factor $g(Z)$ can be applied to all resistances predicted to allow for interference between adjacent flow channels,[8] i.e.,

$$g(Z) = 1 - 1.409Z + 0.296Z^3 \ldots \tag{34}$$

where

$$Z = \frac{\bar{a}_{tot}}{\bar{b}_{tot}} \quad \text{and} \quad \bar{b}_{tot} = \left(\frac{A_N}{\pi\bar{N}_{A_{tot}}A_N}\right)^{0.5} = (\pi\bar{N}_{A_{tot}})^{-0.5} \tag{35}$$

Application of the Prediction

For a given contact assembly, Eq. (13) must be inverted to obtain a normalized prediction mean plane separation t according to the design applied loading pressure P. Then the thickness of the filler to be inserted to minimize the TCR with a pressure P is calculated by plotting and minimizing the TCR as a function of δ.

The Experiments

Specimen Preparation

The contacts were assembled from 12 identical stainless steel cylindrical specimens. All 12 contacting faces (nominally ~0.025 m diam) were ground and lapped in guard holders to within 1 μm flatness and then cleaned with acetone in an ultrasonic machine. The flat surfaces of six of the specimens were subsequently grit-blasted to achieve random surface ordinate distributions. Tin coatings of uniform but different thicknesses were applied to five of the remaining lapped surfaces via a standard ion-plating technique. To ensure a uniform coating thickness on each surface, profilometer tracings were taken after each deposition using as spatial datum points stainless steel bars placed adjacent to the actual specimens during the plating. Microindentation hardness tests were carried out on both the tin-coated surfaces and the clean stainless steel surfaces. Table 1 gives details of the tested assemblies.

Surface Analysis

Measurements of surface roughness, mean surface slope, ordinate distribution, and autocorrelation functions for each

Table 1 Specimen details for the nominally flat contacting surfaces

	Contacting assembly	Coating thickness, μm	Surface roughness, rms, μm	Mean surface slope, deg
1)	U.S.,[a] grit blasted	—	5.220	5.120
	L.S.,[b] lapped	—	0.014	0.064
2)	U.S., grit blasted	—	5.160	5.990
	L.S., lapped and coated	2.8		
3)	U.S., grit blasted	—	5.420	6.120
	L.S., lapped and coated	6.3		
4)	U.S., grit blasted	—	5.820	6.360
	L.S., lapped and coated	12.0		
5)	U.S., grit blasted	—	6.341	6.460
	L.S., lapped and coated	28.0		
6)	U.S., grit blasted	—	6.548	6.670
	L.S., lapped and coated	106.0		

All coated surfaces: rms roughness order of 0.3 μm and mean surface slope 0.9 deg.

Specifications	Specimens: En58b stainless steel	
	Thermal conductivity	$=15.0\ \mathrm{W/m^{-1}K^{-1}}$
	Hardness	$=2\times10^{9}\ \mathrm{Nm^{-2}}$
	Diameter	$=0.025\pm0.001$ m
	Length	$=0.027\pm0.001$ m
Coating	Tin (99.5% purity)	
	Thermal conductivity	$=60.2\ \mathrm{W/m^{-1}K^{-1}}$
	Hardness	$=0.103\times10^{9}\ \mathrm{Nm^{-2}}$

[a] U.S. = upper specimen. [b] L.S. = lower specimen.

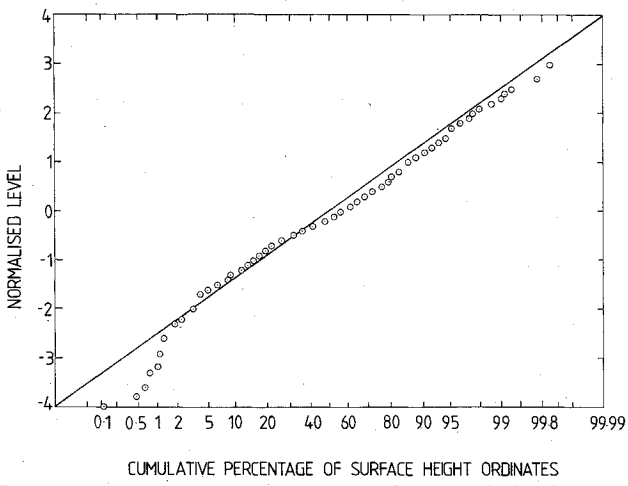

Fig. 2 Normalized height distribution for a typical grit-blasted specimen surface.

specimen surface (prior to being put in contact) were obtained using a Talysurf 4 stylus profilometer. At a sampling interval of 2.822 μm, surface height information for each surface was collected using a microprocessor and then transferred to an interactive computer for evaluation. Details of both the hardware and computer programs used have been described elsewhere.[9-11] Typical ordinate distributions and autocorrelation plots for one of the grit-blasted surfaces are shown in Figs. 2 and 3, respectively.

Thermal Resistances of the Contacts

Experimental measurements of the thermal resistances of the pressed contacts for the assemblies described (see Table 1) were obtained using an evacuated, longitudinal one-dimensional, heat flow system.[4]

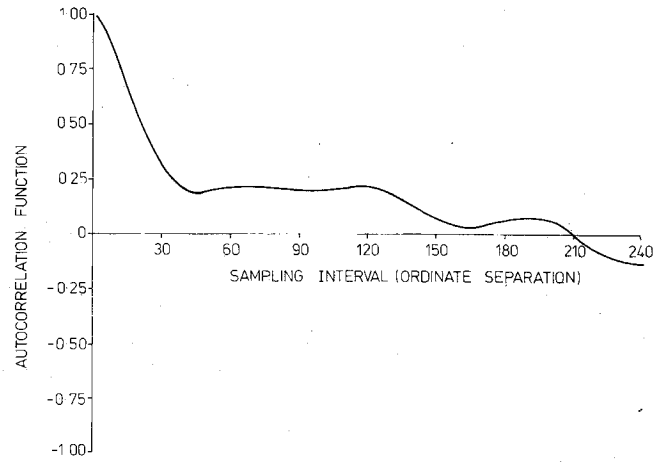

Fig. 3 Autocorrelation function for a typical grit-blasted specimen surface.

The calculation of the average steady-state heat flow $\dot{Q}$ through the contacting specimens was based on the steady-state temperatures recorded by axially placed copper/constantan thermojunctions and the known distance between the thermojunctions. The difference between the extrapolations of the axial temperature profiles so indicated to the interface gave a parameter ΔT, which is known as the average interfacial temperature drop. The total interface resistance R_{tot} is defined as

$$R_{\mathrm{tot}} = \Delta T/\dot{Q} \tag{36}$$

Dynamic vacuums of better than 10^{-4} Torr were maintained and a normal axial heat flux of 5 W was applied for several steady loadings in the range 4.0-22 MN/m^2. The tests started with a small load on the freshly assembled contact, which was increased in increments. The measured mean interfacial temperatures were 47-53°C during the tests.

Experimental Error

The greatest source of experimental error is the fractional error of the measured interfacial temperature drop. This error remains essentially constant for all measurements and thus the percentage compound error associated with the thermal resistance increases as the value of the resistance decreases. This difficulty is inherent in the experimental method employed and is, of course, enhanced when a series of tests covering a wide range of thermal resistance values is performed. Increasing the heat flow to achieve large temperature drops results in larger transverse heat losses from the heater-contacting specimen cooler system. This increases the relative divergence between the true and observed temperature gradients in each test specimen.[12] Therefore, testing at higher power inputs will lead to less accurate experimental results.

The temperature measurement system employed in the Cranfield rig is capable of achieving accuracies to within 0.1°C. Typical compound errors on the thermal contact resistance measurements were 10% for resistances greater than 0.5°C/W, 50% for resistances at 0.1-0.5°C/W, and up to 100% for resistances below 0.1°C/W.

Experimental Measurements—Verification of the Prediction

Figure 4 shows the experimentally obtained data points for the four loads applied and for the range $0<\delta/\sigma<19.4$. The dashed curves join these points, while the solid lines represent the theoretical predictions. The theoretical TCR was assumed to increase linearly from the theoretical minimum resistance calculated according to Eq. (28). The dependencies of the TCR upon applied loading for constant values of δ/σ are given in Fig. 5. Also shown in this figure is the theoretical locus of the minimum TCR. The almost zero values of

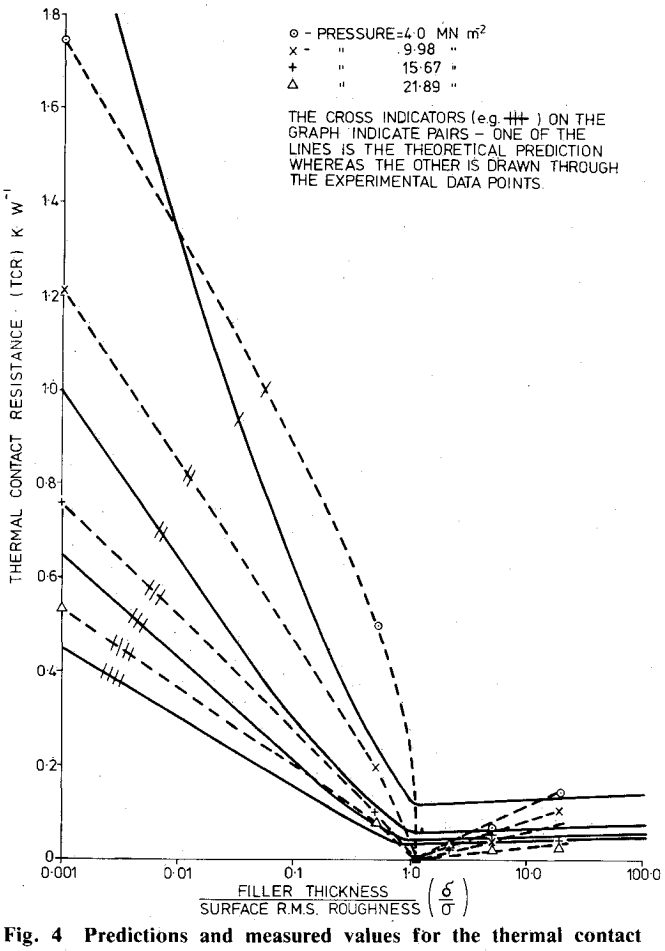

Fig. 4 Predictions and measured values for the thermal contact resistance.

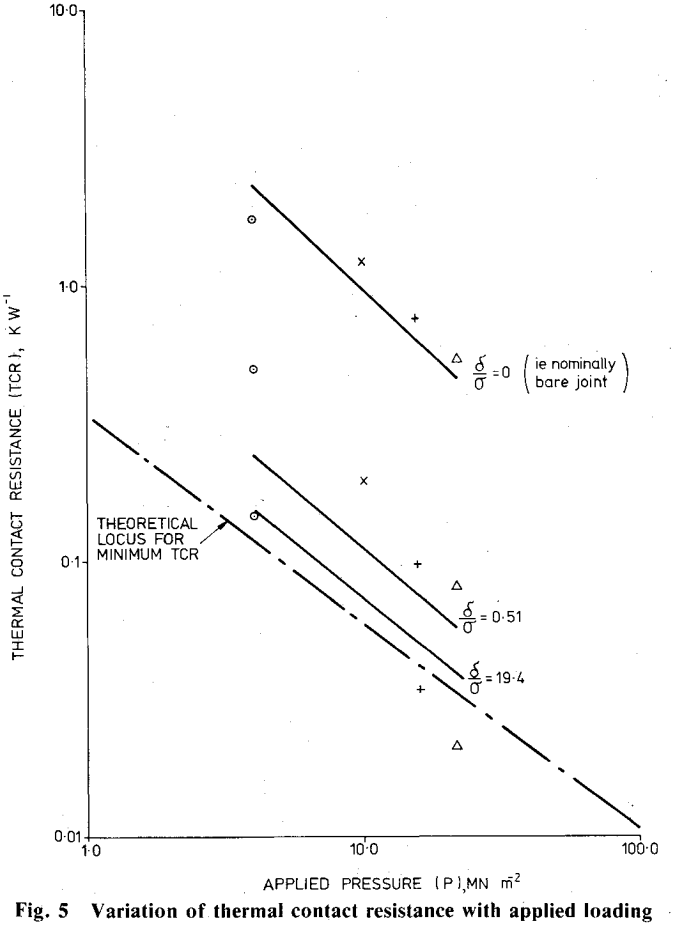

Fig. 5 Variation of thermal contact resistance with applied loading pressure.

resistance measured experimentally for $\delta/\sigma \simeq 1$ have been omitted from this figure.

Discussion

It is certainly evident that increases in coating thickness results in substantial reductions in the TCR until the coating thickness δ approaches the order of σ. *Almost zero values* of TCR were measured for all applied loading when $\delta/\sigma \simeq 1.1$, despite the fact that the prediction suggests higher finite values of TCR that are dependent upon the magnitude of the applied loading. It is apparent that the tin coating employed performed its function in reducing the TCR of the bare joint most successfully. Although the theory predicts very little increase in TCR for $\delta/\sigma > 1.0$ (i.e., any increase corresponding to the resistance of the bulk material), the experiments indicated that greater increased resistances occurred. The reason for this anomaly is not known at this time, but it is suspected that the experimentally observed variations may converge to the theoretical predictions as δ/σ increases outside the range of the data. The major discrepancy is thus the difference between the values of TCR prediction and measured resistance at the optimal value of δ/σ. However, this depends upon the degree of ductility of the coating material. The theory assumes that all the material within the intersections of the contacting surfaces is annihilated. The extrusion of the coating material from these intersections into the noncontact regions lowers the contact resistance, hence the reduced values of TCR observed experimentally. If full, unresisted extrusion occurred, the displaced coating material would completely fill the voids to produce a zero value of contact resistance for a particular applied load and coating thickness. This aspect remains for further theoretical development. The optimal values of δ/σ correspond to the order of those values observed by Yovanovitch.[1]

Conclusions

A theoretical analysis has been developed to predict the optimal soft coating thickness to be applied at a bare joint to result in minimum thermal contact resistance. Freshly measured experimental data corroborate this prediction. The results are in quantitative agreement with observations of previous workers in the field.

Acknowledgments

The authors wish to thank the Science and Engineering Research Council of the United Kingdom for sponsorship of this project.

References

[1] Yovanovitch, M. M., "Investigation of the Effect of Metallic Foils upon Thermal Joint Resistance: Evidence of Optimum Foil Thickness," AIAA Paper 72-283, 1972.

[2] Al-Astrabadi, F. R., O'Callaghan, P. W., Jones, A. M., and Probert, S. D., "Thermal Resistance Resulting from Commonly-Used Inserts Between Stainless Steel Static Surfaces," *Wear*, Vol. 40, No. 3, 1977, pp. 339-350.

[3] Fletcher, L. S. and Miller, R. G., "Thermal Conductance of Gasket Materials for Spacecraft Joints," *AIAA Progress in Astronautics and Aeronautics: Thermophysics and Spacecraft Thermal Control*, Vol. 35, edited by R. G. Hering, MIT Press, Cambridge, Mass., 1974, pp. 335-349.

[4] O'Callaghan, P. W. and Probert, S. D., "Thermal Resistance and Directional Index between Smooth, Non-Wavy Surfaces," *Journal of Mechanical Engineering Science*, Vol. 16, 1974, pp. 41-55.

[5] Al-Astrabadi, F. R., O'Callaghan, P. W., and Probert, S. D., "Effects of Surface Finish on Thermal Contact Resistance between Different Materials," AIAA Paper 79-1065, June 1979.

[6] Al-Astrabadi, F. R., O'Callaghan, P. W., and Probert, S. D., "Thermal Resistance of Contacts—Influence of Oxide Films," AIAA Paper 80-1467, July 1980.

[7]Yip, F. C., "Effect of Oxide Films on Thermal Contact Resistance," *AIAA Progress in Astronautics and Aeronautics: Heat Transfer with Thermal Control Applications*, Vol. 39, edited by M. M. Yovanovitch, MIT Press, Cambridge, Mass., 1975, pp. 45-64.

[8]Roess, L. C., "Theory of Spreading Resistances," Appendix to Weills, N. D. and Ryder, E. A., "Thermal Resistance Measurements on Joints Formed between Stationary Metal Surfaces," Paper presented at Semi-Annual Meeting, ASME Heat Transfer Division, Milwaukee, 1948.

[9]Edmonds, M. J., Snaith, B., and Probert, S. D., "A Practical Means of Quantitatively Describing the Topographies of Machined Surfaces," *Transactions of Institute of Measurement and Control*, Vol. 2, No. 3, July-Sept. 1980, pp. 157-163.

[10]Snaith, B., Edmonds, M. J., and Probert, S. D., "Use of Profilometer for Surface Mapping," *Precision Engineering*, Vol. 3, No. 2, April 1981, pp. 87-90.

[11]O'Callaghan, P. W., "Some Aspects of Contacts between Solids," Ph.D. Thesis, University of Wales, United Kingdom, Aug. 1971.

[12]O'Callaghan, P. W. and Probert, S. D., "The Effects of Transverse Heat Losses on Longitudinal Heat Transport Observations," *Measurement and Control*, Vol. 4, March 1971, pp. 25-34.

From the AIAA Progress in Astronautics and Aeronautics Series

RAREFIED GAS DYNAMICS—v. 74 (Parts I and II)

Edited by Sam S. Fisher, University of Virginia

The field of rarefied gas dynamics encompasses a diverse variety of research that is unified through the fact that all such research relates to molecular-kinetic processes which occur in gases. Activities within this field include studies of (a) molecule-surface interactions, (b) molecule-molecule interactions (including relaxation processes, phase-change kinetics, etc.), (c) kinetic-theory modeling, (d) Monte-Carlo simulations of molecular flows, (e) the molecular kinetics of species, isotope, and particle separating gas flows, (f) energy-relaxation, phase-change, and ionization processes in gases, (g) molecular beam techniques, and (h) low-density aerodynamics, to name the major ones.

This field, having always been strongly international in its makeup, had its beginnings in the early development of the kinetic theory of gases, the production of high vacuums, the generation of molecular beams, and studies of gas-surface interactions. A principal factor eventually solidifying the field was the need, beginning approximately twenty years ago, to develop a basis for predicting the aerodynamics of space vehicles passing through the upper reaches of planetary atmospheres. That factor has continued to be important, although to a decreasing extent; its importance may well increase again, now that the USA Space Shuttle vehicle is approaching operating status.

A second significant force behind work in this field is the strong commitment on the part of several nations to develop better means for enriching uranium for use as a fuel in power reactors. A third factor, and one which surely will be of long term importance, is that fundamental developments within this field have resulted in several significant spinoffs. A major example in this respect is the development of the nozzle-type molecular beam, where such beams represent a powerful means for probing the fundamentals of physical and chemical interactions between molecules.

Within these volumes is offered an important sampling of rarefied gas dynamics research currently under way.The papers included have been selected on the basis of peer and editor review, and considerable effort has been expended to assure clarity and correctness.

1248 pp., 6×9, illus., $55.00 Mem., $95.00 List

TO ORDER WRITE: Publications Order Dept., AIAA, 1633 Broadway, New York, N.Y. 10019